Cavity Optomechanical Sensing and Manipulation of an Atomic Persistent Current

Pardeep Kumar, Tushar Biswas, Kristian Feliz, Rina Kanamoto, M.-S. Chang, Anand K. Jha, and M. Bhattacharya

Phys. Rev. Lett. **127**, 113601 — Published 9 September 2021

DOI: 10.1103/PhysRevLett.127.113601

Cavity Optomechanical Sensing and Manipulation of an Atomic Persistent Current

Pardeep Kumar,[1,*] Tushar Biswas,[1] Kristian Feliz,[1] Rina Kanamoto,[2] M.-S. Chang,[3,4] Anand K. Jha,[5] and M. Bhattacharya[1]

[1]*School of Physics and Astronomy, Rochester Institute of Technology, 84 Lomb Memorial Drive, Rochester, NY 14623, USA*
[2]*Department of Physics, Meiji University, Kawasaki, Kanagawa 214-8571, Japan*
[3]*Institute of Atomic and Molecular Sciences, Academia Sinica, Taipei, 10617, Taiwan*
[4]*Department of Physics and Center for Quantum Technology, National Tsing Hua University, Hsinchu, 30013, Taiwan*
[5]*Department of Physics, Indian Institute of Technology, Kanpur, UP, 208016, India*

(Dated: August 17, 2021)

Abstract

This theoretical work initiates contact between two frontier disciplines of physics, namely atomic superfluid rotation and cavity optomechanics. It considers an annular Bose-Einstein condensate (BEC), which exhibits dissipationless flow and is a paradigm of rotational quantum physics, inside a cavity excited by optical fields carrying orbital angular momentum (OAM). It provides the first platform that can sense ring BEC rotation with minimal destruction, *in situ* and in real time, unlike demonstrated techniques, all of which involve fully destructive measurement. It also shows how light can actively manipulate rotating matter waves by optomechanically entangling persistent currents. Our work opens up a novel and useful direction in the sensing and manipulation of atomic superflow.

PACS numbers: 42.50.-p, 37.30.+i, 37.10Vz,03.75.Gg

Introduction.– Persistent currents in annularly-trapped atomic superfluids [1, 2] offer a highly controllable laboratory for studying phenomena associated with quantum circulation, such as phase slips [3–6], hysteresis [7], shock waves [8], matter-wave interferometry [9], gyroscopy [10–12], atomtronic circuits [13], Josephson physics [14], time crystals [15], topological excitations [16, 17] and cosmological simulations [18]. All these works rely on the fact that a BEC confined on a ring - unlike one contained in a simply-connected trap [19–21] - can support vortices for macroscopically long times [1].

Characterizing the rotational state of a ring BEC is therefore of fundamental importance, with implications for several areas of physics. In this context it is essential to note that the information about the angular momentum of a BEC in a rotational eigenstate is carried in its phase (in the form of its winding number) and not in its density profile, which remains uniform around the ring. However, all methods sensitive to the BEC winding number demonstrated so far involve absorption imaging of the atoms in the ring and are therefore fully destructive of the condensate [1, 2, 4, 9, 13, 18, 22].

On the other hand, minimally destructive detection by removing a few atoms from the BEC for each measurement [23], or nondestructive imaging using light far off-resonance on an atomic transition [24], are only sensitive to the atomic density and not to the BEC phase. Such experiments in fact rely on measuring vortex precession in order to infer the BEC angular momentum. But this technique cannot be used on an annularly trapped BEC, as a vortex on a ring does not precess, since its core is pinned to the ring center. The difficulties enumerated so far may be overcome, in principle, by non-destructively tracking superfluid rotation by off-resonantly imaging a precessing density modulation impressed on the condensate [25], or by continuously monitoring the number of atoms tunneling out from the ring [26]. Detection of more involved properties of the rotating condensate, such as entanglement, however, involve destructive protocols exclusively [11, 27].

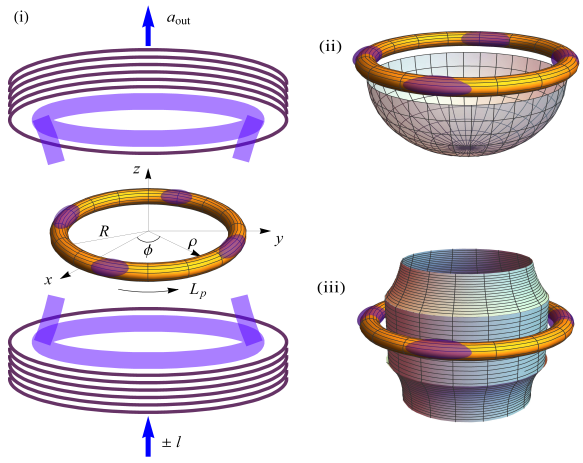

FIG. 1. BEC with winding number L_p rotating in a ring trap of radius R, probed by modes carrying OAM $\pm l\hbar$ in a (i) Fabry-Perot cavity with transmitted field $a_{\rm out}$ (ii) hemispherical cavity, and (iii) bottle-shaped optical microresonator. Shaded regions of the ring correspond to intensity maxima of the optical modes for $l = 2$.

In this Letter we propose to solve the outstanding problems related to the measurement of ring BEC rota-

tion by exploiting the techniques of cavity optomechanics, a versatile paradigm for sensing the motion of mechanically pliable objects based on their interaction with electromagnetic fields confined to an optical resonator [28–31].

Setup.—The configuration of interest is shown in Fig. 1(i), [variations on the basic geometry are displayed in Figs. 1(ii) and (iii), respectively] namely, an atomic (e.g. Sodium) BEC confined in a toroidal trap [32–36] located at the center of an optical cavity. The potential experienced by each atom of mass m in the condensate is [35]

$$U(\rho,z)=\frac{1}{2}m\omega_\rho(\rho-R)^2+\frac{1}{2}m\omega_z z^2, \tag{1}$$

where ω_ρ and ω_z are the harmonic trapping frequencies along the radial and axial directions, respectively and R is the radius of the ring trap. In the potential $U(\rho,z)$ the dynamics along the radial (ρ), axial (z) and azimuthal (ϕ) directions decouple. We assume that all atoms remain in the same quantum state along the radial and axial directions during dynamical evolution; we focus instead on the azimuthal motion of the atoms, i.e. along ϕ, which is not subject to any trapping.

This one-dimensional description is within reach of state-of-the-art laboratories [36], has been successful in modeling experiments which include radial degrees of freedom [4, 17, 37], and applies if [35]

$$N<\frac{4\sqrt{\pi}R}{3a_{\rm Na}}\left(\frac{\omega_\rho}{\omega_z}\right)^{1/2}, \tag{2}$$

where N and $a_{\rm Na}$ are the number and ground state scattering length of the Sodium atoms in the condensate, respectively.

A superposition of two frequency-degenerate optical beams derived from the same laser and carrying OAM $\pm l\hbar$ is now injected into the cavity to probe the BEC. Such coherent superpositions have been experimentally demonstrated to create an angular lattice inside the cavity about its axis [38]. The beams are blue detuned far from the ground-to-excited state atomic transition and therefore interact weakly with the atoms via the dipole force, with the effect of spontaneous photon scattering being negligible. Photon decay from the cavity will be accounted for below.

The azimuthal motion of the BEC is described, in the frame rotating at the laser drive frequency, by the one-dimensional Hamiltonian [39, 48–50]

$$\begin{aligned}H=&\int_0^{2\pi}\Psi^\dagger(\phi)\left[-\frac{\hbar^2}{2I}\frac{d^2}{d\phi^2}+\hbar U_o\cos^2(l\phi)\,a^\dagger a\right]\Psi(\phi)d\phi\\&+\frac{g}{2}\int_0^{2\pi}\Psi^\dagger(\phi)\Psi^\dagger(\phi)\Psi(\phi)\Psi(\phi)d\phi\\&-\hbar\Delta_o a^\dagger a-i\hbar\eta(a-a^\dagger),\end{aligned} \tag{3}$$

where the bosonic atomic field operators obey $[\Psi(\phi),\Psi^\dagger(\phi')]=\delta(\phi-\phi')$ and the photonic operators follow $[a,a^\dagger]=1$. The first term in the bracket on the first line of Eq. (3) represents the rotational kinetic energy of the atoms, with $I=mR^2$ the atomic moment of inertia about the cavity axis. The second term in the bracket describes the interaction of the atoms with the optical lattice such that $U_o=g_a^2/\Delta_a$, where g_a is the strength of the interaction between one photon and one atom and Δ_a is the detuning of the optical frequency from the atomic transition. The second line of Eq. (3) represents two-body atomic interactions, with strength $g=2\hbar\omega_\rho a_{\rm Na}/R$ [35, 50]. The first term in the third line of Eq. (3) is the cavity field energy in the rotating frame of the drive; the detuning $\Delta_{\rm o}$ equals the driving field frequency minus the cavity resonance ω_o. The last term of Eq. (3) is due to the cavity drive and $\eta=\sqrt{P_{\rm in}\gamma_o/\hbar\omega_o}$ where $P_{\rm in}$ is the optical power and γ_o is the cavity linewidth.

The condensate may be set to rotation using a variety of techniques, including optical stirring [1, 2, 4], employing radio-frequency fields [33] or via quenching [17] to impart a winding number L_p to the BEC. We do not consider further the details of this process as they are well-addressed in the literature, and as our main task in the present work is to measure the condensate winding number L_p (and thus the angular momentum $\Lambda=\hbar L_p$).

Let us now consider the relevant physical processes in our system. The presence of the optical lattice causes some atoms in the condensate to coherently Bragg scatter [22] from their rotational state with winding number L_p to states with $L_p\pm 2nl$, where $n=1,2,3,\ldots$. The linear analog of such matter-wave scattering from an optical lattice inside a cavity has already been demonstrated in Ref. [48]. We assume the dipole potential to be weak (i.e. smaller than the chemical potential of the rotating condensate), and in that case the number of atoms scattered is small and only first order diffraction, $L_p\to L_p\pm 2l$, is appreciable.

Based on this physical picture, we propose an *ansatz* for the atomic field

$$\Psi(\phi)=\frac{e^{iL_p\phi}}{\sqrt{2\pi}}c_p+\frac{e^{i(L_p+2l)\phi}}{\sqrt{2\pi}}c_++\frac{e^{i(L_p-2l)\phi}}{\sqrt{2\pi}}c_-, \tag{4}$$

where the atomic operators obey $[c_i,c_j^\dagger]=\delta_{ij}$, $(i,j)=p,+,-$, and $c_p^\dagger c_p+c_+^\dagger c_++c_-^\dagger c_-=N$. The first term in Eq. (4) corresponds to the original persistent current and the remaining two terms are the sidemodes excited by matter wave diffraction. However, since the number of atoms in the sidemodes is small, and the mode with winding number L_p is macroscopically occupied (i.e. its dynamics are classical), we posit $c_p^\dagger c_p\simeq N$ and introduce the operators $c=c_p^\dagger c_+/\sqrt{N}$ and $d=c_p^\dagger c_-/\sqrt{N}$, where $c_p^\dagger$ is now a complex number. Using these relations and

Eq. (4) in Eq. (3) we get, neglecting all constant terms,

$$H = \hbar\omega_c c^\dagger c + \hbar\omega_d d^\dagger d + \hbar\left[G(X_c + X_d) - \tilde{\Delta}\right] a^\dagger a \\ -i\hbar\eta(a - a^\dagger) + \hbar\tilde{g}\tilde{C}, \quad (5)$$

where $G = U_o\sqrt{N}/2\sqrt{2}$, $\tilde{\Delta} = \Delta_o - U_o N/2$, $\tilde{g} = g/(4\pi\hbar)$, $X_c = (c^\dagger + c)/\sqrt{2}$, and $X_d = (d^\dagger + d)/\sqrt{2}$.

The sidemodes are particle-like excitations of the condensate and therefore their frequencies

$$\omega_c = \frac{\hbar(L_p + 2l)^2}{2I}, \ \omega_d = \frac{\hbar(L_p - 2l)^2}{2I}, \quad (6)$$

are quadratic in the respective angular momenta. A full Bogoliubov analysis actually yields the sidemode frequencies $\omega'_{c,d} = [\omega_{c,d}(\omega_{c,d} + 4\tilde{g}N)]^{1/2}$ [51]. Here, for simplicity, we ensure $\omega_{c,d} \gg 4\tilde{g}N$ such that $\omega'_{c,d} \simeq \omega_{c,d}$. Similar particle-like excitations were earlier created in a linear analog of our proposal [48, 52]. Finally, $\hbar\tilde{g}\tilde{C}$ in Eq. (5) represents the effect of atomic interactions. In the Supplementary Material (SM) [39] we have provided the full expression for $\tilde{C}$ and shown that its presence does not essentially affect our proposed protocol, even though it slightly modifies Eqs. (6), for example.

Neglecting $\hbar\tilde{g}\tilde{C}$, the right hand side of Eq. (5) has the form of the canonical optomechanical Hamiltonian, coupling the displacement (e.g. X_c, X_d) of one or more mechanical oscillators to the cavity photon number $a^\dagger a$ [28]. The corresponding ($\tilde{g} \equiv 0$) equations of motion are

$$\ddot{X}_c + \gamma_m \dot{X}_c + \omega_c^2 X_c = -\omega_c G a^\dagger a + \omega_c \epsilon_c, \quad (7)$$

$$\ddot{X}_d + \gamma_m \dot{X}_d + \omega_d^2 X_d = -\omega_d G a^\dagger a + \omega_d \epsilon_d, \quad (8)$$

$$\dot{a} = i\left[\tilde{\Delta} - G\left(X_c + X_d\right)\right] a - \frac{\gamma_o}{2} a + \eta + \sqrt{\gamma_o} a_{\rm in}, \quad (9)$$

where dissipation and noise have been introduced according to the standard quantum Langevin formalism [28], and the damping of each condensate sidemode (assumed to be the same for simplicity) is γ_m [1, 3]. The mechanical and optical fluctuations have zero mean ($\langle\epsilon_c\rangle = \langle\epsilon_d\rangle = \langle a_{\rm in}\rangle = 0$); their correlations will be specified below.

Rotation sensing.—The basic physics underlying our proposal for sensing of atomic rotation can be readily understood from a heuristic discussion of Eqs. (7)-(9). Neglecting damping and noise, and for weak optical driving, Eqs. (7) and (8) imply that X_c and X_d oscillate at frequencies ω_c and ω_d, respectively. From Eq. (9) we can then see that the cavity optical field is also modulated at these two mechanical frequencies. Physically, this modulation is due to the density variations in the BEC caused by atom scattering from the optical lattice; the effect may also be understood as a rotational Doppler shift imprinted on the cavity photons by the circulating atoms [53]. A homodyne measurement of the cavity output field $a_{\rm out} = -a_{\rm in} + \sqrt{\gamma_o} a$ [28] (also see Fig. 1), should therefore reveal the frequencies $\omega_{c,d}$ and thus also the winding number of the condensate L_p, since in experiments l and I are known parameters. To confirm quantitatively the above heuristic arguments, we now present the linear response of our system taking quantum noise and damping into account.

We start with the steady state solutions to Eqs. (7)-(9), which are $X_{c,s} = -G|a_s|^2/\omega_c, X_{d,s} = -G|a_s|^2/\omega_d$, and $a_s = -\eta/(i\Delta' - \gamma_o/2)$, where $\Delta' = \tilde{\Delta} + G^2|a_s|^2\Omega$ and $\Omega = (\omega_c + \omega_d)/\omega_c\omega_d$. As in conventional optomechanics, these solutions display bistability, see Fig. 2 [28, 48]. We note that these bistability curves will likely undergo small shifts due to coherent non-steady state dynamics [54]. However, our aim is only to establish approximately the threshold of bistability, and our rotation measurement (and entanglement generation) will be carried out using parameters which keep the system monostable (such that the non-steady-state dynamics are negligible) and thus orders of magnitude below the bistable regime.

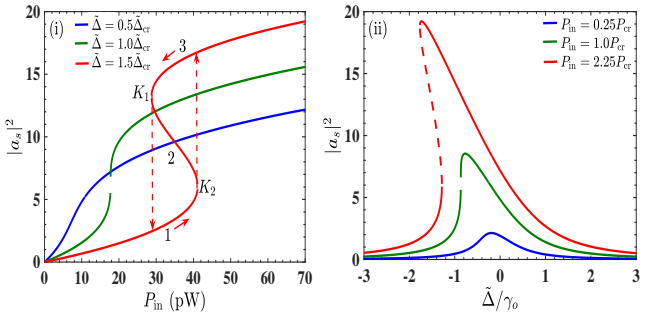

FIG. 2. Optomechanical bistability. (i) Intracavity photon number versus cavity drive power for several effective cavity detunings. Bistability occurs above $\tilde{\Delta}_{\rm cr}/2\pi = -1.73$ MHz, and between K_1 and K_2, with the stable branches labeled as 1 and 3. (ii) Intracavity photon number versus effective cavity detuning for various values of $P_{\rm in}$, where bistability appears at $P_{\rm cr} = 17.7$ pW. Parameters used are $m = 23$ amu, $R = 12$ μm, $N = 10^4$, $G/2\pi = 7.5$ kHz, $L_p = 1$, $l = 10$, $\Delta_a/2\pi = 4.7$ GHz, $\omega_z/2\pi = 42$ Hz, $\omega_\rho/2\pi = 42$ Hz, $\gamma_m/2\pi = 0.8$ Hz, $\gamma_o/2\pi = 2$ MHz, and $\omega_o/2\pi = 10^{15}$ Hz.

To obtain the linear response, we write each variable in Eqs. (7)-(9) as the sum of the steady state value and a small fluctuation, i.e. $\mathcal{M} \to \mathcal{M}_s + \delta\mathcal{M}$ for $\mathcal{M} = X_c, X_d, a$, and obtain the linearized equations as $\dot{u}(t) = Fu(t) + v(t)$, with $u(t) = [\delta X_c(t), \delta Y_c(t), \delta X_d(t), \delta Y_d(t), \delta Q(t), \delta P(t)]^T$, $v(t) = \left[0, \epsilon_c(t), 0, \epsilon_d(t), \sqrt{\gamma_o}\delta Q_{\rm in}(t), \sqrt{\gamma_o}\delta P_{\rm in}(t)\right]^T$, $Y_c = i(c^\dagger - c)/\sqrt{2}, Y_d = i(d^\dagger - d)/\sqrt{2}, Q = (a^\dagger + a)/\sqrt{2}, P = i(a^\dagger - a)/\sqrt{2}$, where the matrix F is provided in the SM [39]. Fourier transforming, we now consider the homodyne measurement of the fluctuations $\delta\mathcal{P}_{\rm out}(\omega)$ in the cavity output phase quadrature (where ω is the system response frequency) $\mathcal{P}_{\rm out}(\omega) = i[a^\dagger_{\rm out}(\omega) - a_{\rm out}(\omega)]/\sqrt{2}$.

Choosing without loss of generality the cavity drive phase such that a_s is real, using the noise correlations

$\langle a_{\rm in}(\omega)a^{\dagger}_{\rm in}(\omega')\rangle = 2\pi\delta(\omega+\omega')$, and

$$\langle \epsilon_c(\omega)\epsilon_c(\omega')\rangle = \frac{2\pi\gamma_m\omega}{\omega_c}\left[1+\coth\left(\frac{\hbar\omega}{2k_BT}\right)\right]\delta(\omega+\omega'), \tag{10}$$

and similarly for the other sidemode, and employing standard methods, we obtain the quadrature noise spectrum [28]

$$S(\omega) = S_{\rm sn}(\omega) + S_{\rm rp}(\omega) + S_{\rm th}(\omega). \tag{11}$$

The first two terms in Eq. (11) describe the shot noise $S_{\rm sn}(\omega) = [\omega^2 + (\gamma_o^2/4)]/4\gamma_o G^2 a_s^2$ and radiation pressure contributions $S_{\rm rp}(\omega) = \gamma_o G^2 a_s^2 \mathcal{F}(\omega)/(\omega^2+\gamma_o^2/4)$, respectively, with

$$\mathcal{F}(\omega) = \Omega^2|\omega_c\chi_c(\omega)|^2|\omega_d\chi_d(\omega)|^2\left[\left(\omega^2-\omega_c\omega_d\right)^2+\gamma_m^2\omega^2\right], \tag{12}$$

where $\chi_{c,d}(\omega) = (\omega_{c,d}^2 - \omega^2 - i\omega\gamma_m)^{-1}$ are the sidemode susceptibilities. The final term in Eq. (11)

$$S_{\rm th}(\omega) = \gamma_m\omega\left[\omega_c|\chi_c(\omega)|^2 + \omega_d|\chi_d(\omega)|^2\right]\coth\left(\frac{\hbar\omega}{2k_BT}\right), \tag{13}$$

is due to mechanical fluctuations.

Plotting $S(\omega)$ as a function of system response frequency ω [Fig. 3(i)], we clearly see the peaks expected

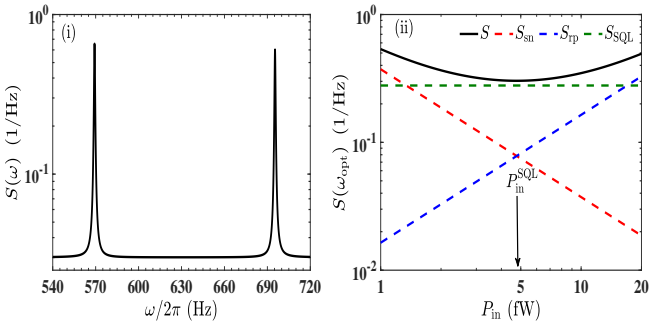

FIG. 3. Noise spectrum (i) $S(\omega)$ versus response frequency $\omega/2\pi$ for $P_{\rm in} = 12.4$ fW; the peaks at $\omega_d/2\pi = 569$ Hz and $\omega_c/2\pi = 695$ Hz correspond to $L_p = 1$ and $l = 10$ (ii) $S(\omega_{\rm opt})$ versus input power $P_{\rm in}$, where $\omega_{\rm opt}/2\pi = \omega_c/2\pi + 0.3$ Hz [see inset of Fig. 4(i)]. The red (blue) straight dashed line with a negative (positive) slope indicates optical shot (radiation pressure) noise. Here, $\Delta' = 0$ and $P_{\rm in}^{\rm SQL} = 4.8$ fW. The remaining parameters are, in addition to $T = 20$ nK, the same as in Fig. 2.

at ω_c and ω_d, respectively. We have confirmed that L_p can be accurately extracted from these peaks, for various sets of parameters, thus verifying our conjecture that the cavity transmission indicates atomic rotation. We note from Eqs. (7) and (8) that for $(L_p, l) \neq 0$, it follows that $\omega_c \neq \omega_d$ and therefore the coupling of the sidemodes to the cavity photon number is unequal. This observation underlies the slight peak asymmetry observed in Fig. 3(i). Plotting $S(\omega)$ as a function of cavity drive power $P_{\rm in}$ [Fig. 3(ii)] shows the existence of a standard quantum limit where the combined effect of the shot noise and radiation pressure noise is minimized for an optimum power $P_{\rm in}^{\rm SQL}$, as in standard cavity optomechanics [28].

We now characterize the rotation measurement sensitivity quantitatively. In the regime of linear response it is given by [55]

$$\zeta = \frac{S(\omega)}{\partial S(\omega)/\partial\Lambda}\times\sqrt{t_{\rm meas}}, \tag{14}$$

where $t_{\rm meas}^{-1} \simeq 8(a_sG)^2/\gamma_o$ is the optomechanical measurement rate in the bad cavity limit ($\omega_{c,d} \ll \gamma_o$) applicable to our system [28]. The change in the sensitivity with various parameters is shown in Fig. 4. The best sensitivity occurs at frequencies ω_c and ω_d, respectively, when the sidemode mechanical susceptibilities peak [Fig. 4(i)]; also, the sensitivity improves with l as more optical lattice sites interact with the BEC [Fig. 4(ii)].

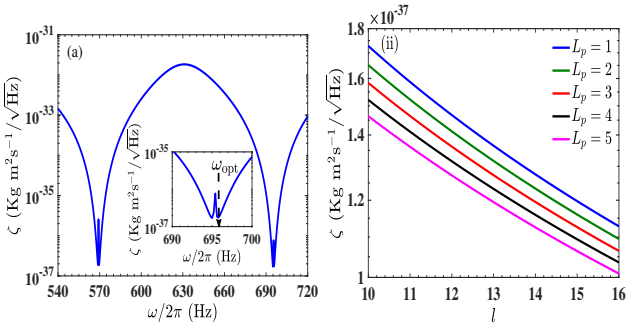

FIG. 4. Rotation sensitivity versus (i) response frequency $\omega/2\pi$ and (ii) OAM number l. Here $P_{\rm in} = 12.4$ fW and the remaining parameters are the same as in Fig. 2 except in (ii) $\omega = \omega_{\rm opt}$.

For realistic parameters we find that the best sensitivity of our method to the rotation of a BEC with respect to a stationary laboratory is $\sim 10^{-3}{\rm Hz}/\sqrt{\rm Hz}$, three orders of magnitude better than demonstrated thus far [25] and comparable to theoretical proposals based on fully destructive measurements [12]. Also, for our parameters, the optomechanical measurement time $t_{\rm meas} \simeq 60$ ms is shorter than the orbital period of an atom (~ 300 ms for $L_p = 1$) around the ring trap, much shorter than the duration of a persistent current ($\sim$ seconds [2, 3], thus making the measurement practically real time), and very much shorter than the photon scattering time ($\sim$ minutes). Finally, we note that our scheme for measuring L_p only requires a few atoms to be removed from the original persistent current mode - but not from the ring trap - into the sidemodes, and is therefore minimally destructive [23].

Optomechanical entanglement.— To demonstrate that our proposed platform enables not only passive measurement but also active manipulation of persistent currents, we now show that light can optomechanically entangle

the two rotating matter wave sidemodes. This could be useful for rotating matter waves to serve as a memory for OAM-carrying photons, which are of current interest for the large Hilbert space they offer for quantum information processing purposes [27, 56].

We use the experimentally accessible logarithmic negativity $\mathcal{E}_{\mathcal{N}} = \max[0, -\ln(2\sigma_-)]$ [28, 57], as a measure of bipartite entanglement, where $\sigma_- = 2^{-1/2}\left[\Sigma - \sqrt{\Sigma^2 - 4\det(V_{\rm sub})}\right]^{1/2}, \Sigma = \det A + \det B - 2\det C$, and $V_{\rm sub} = ((A, C), (C^T, B))$ is the covariance matrix provided in the SM [39]. Entanglement between the two sidemodes turns on when optical interaction with the matter waves, proportional to the number of lattice maxima $2l$, becomes frequent enough [Fig. 5(i)] and degrades with temperature [Fig. 5(ii)]. A systematic study of the effect of atomic interactions on all results has been provided in the SM [39].

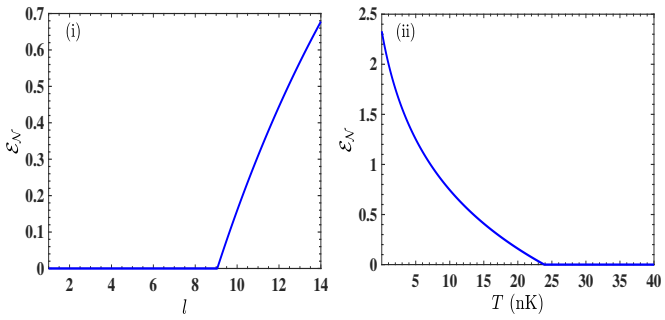

FIG. 5. Bipartite entanglement between two sidemodes versus (i) OAM number l for $T = 20$ nK and (ii) temperature T for $l = 10$. Except for $\Delta' = \omega_c$, and $P_{\rm in} = 0.4$ fW, the parameters are the same as in Fig. 2.

Conclusion.— We have proposed a method of measuring the rotation of a ring BEC by coupling it to orbital angular momentum-carrying beams inside an optical cavity. For realistic parameters this method improves upon currently available rotation sensitivities by three orders of magnitude. Our proposal also advances the frontier of optomechanics from the paradigm of light fields interacting with mechanical vibrations to include coherent atomic rotation, thus opening up the possibility of using rotating matter waves to realize applications such as storage and retrieval of information. Future work will consider more complex many-body states, vortex nucleation and decay, and gauge fields.

TB, KF and MB are grateful to the NSF, Directorate for Mathematical and Physical Sciences for support (1454931). RK is supported by JST, CREST Grant No. JPMJCR1771, and JSPS KAKENHI Grant No. JP21K03421. MSC thanks MoST of Taiwan with Grant No. 106-2112-M-001-033. AKJ acknowledges financial support through research grant no. EMR/2015/001931 from SERB, DST, Govt. of India. PK has been supported in part by the Grant No. CMMI 1661618 from the National Science Foundation. The authors thank R. Wilson, S. Ghosh and H. Wanare for useful discussions.

* mehra.pardeep89@gmail.com

[1] C. Ryu, M. F. Andersen, P. Clade, V. Natarajan, K. Helmerson, and W. D. Phillips, Observation of persistent flow of a Bose-Einstein condensate in a toroidal trap, Phys. Rev. Lett. **99**, 260401 (2007).
[2] S. Beattie, S. Moulder, R. J. Fletcher, and Z. Hadzibabic, Persistent currents in spinor condensates, Phys. Rev. Lett. **110**, 025301 (2013).
[3] S. Moulder, S. Beattie, R. P. Smith, N. Tammuz, and Z. Hadzibabic, Quantized supercurrent decay in an annular Bose-Einstein condensate, Phys. Rev. A **86**, 013629 (2012).
[4] K. C. Wright, R. B. Blakestad, C. J. Lobb, W. D. Phillips,and G. K. Campbell, Driving phase slips in a superfluid atom circuit with a rotating weak link, Phys. Rev. Lett. **110**, 025302 (2013).
[5] K. Snizhko, K. Isaieva, Y. Kuriatnikov, Y. Bidasyuk, S. Vilchinskii, and A. Yakimenko, Stochastic phase slips in toroidal Bose-Einstein condensates, Phys. Rev. A **94**, 063642 (2016).
[6] R. Kanamoto, L. D. Carr, and M. Ueda, Topological winding and unwinding in metastable Bose-Einstein condensates, Phys. Rev. Lett. **100**, 060401 (2008).
[7] S. Eckel, J. G. Lee, F. Jendrzejewski, N. Murray, C. W. Clark, C. J. Lobb, W. D. Phillips, M. Edwards, and G. K. Campbell, Hysteresis in a quantized superfluid 'atomtronic' circuit, Nature **506**, 200 (2014).
[8] Y. H. Wang, A. Kumar, F. Jendrzejewski, R. M. Wilson, M. Edwards, S. Eckel, G. K. Campbell, and C. W. Clark, Resonant wavepackets and shock waves in an atomtronic SQUID, New J. Phys. **17**, 125012 (2015).
[9] G. E. Marti, R. Olf, and D. M. Stamper-Kurn, Collective excitation interferometry with a toroidal Bose-Einstein condensate, Phys. Rev. A **91**, 013602 (2015).
[10] G. Pelegri, J. Mompart, and V. Ahufinger, Quantum sensing using imbalanced counter-rotating Bose-Einstein condensate modes, New J. Phys. **20**, 103001 (2018).
[11] J. J. Cooper, D. W. Hallwood, and J. A. Dunningham, Entanglement-enhanced atomic gyroscope, Phys. Rev. A **81**, 043624 (2010).
[12] S. Ragole, and J. M. Taylor, Interacting atomic interferometry for rotation sensing approaching the Heisenberg limit, Phys. Rev. Lett **117**, 203002 (2016).
[13] A. Ramanathan, K. C. Wright, S. R. Muniz, M. Zelan, W. T. Hill III, C. J. Lobb, and K. Helmerson, Superflow in a toroidal Bose-Einstein condensate: an atom circuit with a tunable weak link, Phys. Rev. Lett. **106**, 130401 (2011).
[14] C. Ryu, P. W. Blackburn, A. A. Blinova, and M. G. Boshier, Experimental realization of Josephson junctions for an atom SQUID, Phys. Rev. Lett. **111**, 205301 (2013).
[15] P. Öhberg, and E. W. Wright, Quantum Time Crystals and Interacting Gauge Theories in Atomic Bose-Einstein Condensates, Phys. Rev. Lett. **123**, 250402 (2019).
[16] A. Das, J. Sabbatini, and W. H. Zurek, Winding up superfluid in a torus via Bose Einstein condensation, Sci-

entific Reports **2**, 352 (2012).
[17] L. Corman, L. Chomaz, T. Bienaime, R. Desbuquois, C. Weitenberg, S. Nascimbene, J. Dalibard, and J. Beugnon, Quench-induced supercurrents in an annular Bose gas, Phys. Rev. Lett. **113**, 135302 (2014).
[18] S. Eckel, A. Kumar, T. Jacobson, I. B. Spielman, and G. K. Campbell, A rapidly expanding Bose-Einstein condensate: an expanding universe in the lab, Phys. Rev. X **8**, 021021 (2018).
[19] D. S. Rokhsar, Vortex stability and persistent currents in trapped Bose gases, Phys. Rev. Lett.**79**, 2164 (1997).
[20] A. Fetter, Rotating trapped Bose-Einstein condensates, Rev. Mod. Phys. **81** 647 (2009).
[21] B. P. Anderson, Resource article: Experiments with vortices in superfluid atomic gases, J. Low. Temp. Phys. **161**, 574 (2010).
[22] S. R. Muniz, D. S. Naik, and C. Raman, Bragg spectroscopy of vortex lattices in Bose-Einstein condensates, Phys. Rev. A **73**, 041605R (2006).
[23] D. V. Freilich, D. M. Bianchi, A. M. Kaufman, T. K. Langin, and D. S. Hall, Real-time dynamics of single vortex lines and vortex dipoles in a Bose-Einstein condensate, Science **329**, 1182 (2010).
[24] B. P. Anderson, P. C. Haljan, C. E. Wieman, and E. Cornell, Vortex precession in Bose-Einstein condensates: observations with filled and empty cores, Phys. Rev. Lett. **85**, 2857 (2000).
[25] A. Kumar, N. Anderson, W. D. Phillips, S. Eckel, G. K. Campbell, and S. Stringari, Minimally destructive, Doppler measurement of a quantized flow in a ring-shaped Bose-Einstein condensate, New J. Phys. **18**, 025001 (2016).
[26] S. Safaei, L. C. Kwek, R. Dumke, and L. Amico, Monitoring currents in cold-atom circuits, Phys. Rev. A **100**, 013621 (2019).
[27] N. L. Gullo, S. McEndoo, T. Busch, and M. Paternostro, Vortex entanglement in Bose-Einstein condensates coupled to Laguerre-Gauss beams, Phys. Rev. A **81**, 053625 (2010).
[28] M. Aspelmeyer, T. J. Kippenberg, and F. Marquardt, Cavity optomechanics, Rev. Mod. Phys. **86**, 1391 (2014).
[29] L. Childress, M. P. Schmidt, A. D. Kashkanova, C. D. Brown, G. I. Harris, A. Aiello, F. Marquardt, and J. G. E. Harris, Cavity optomechanics in a levitated helium drop, Phys. Rev. A **96**, 063842 (2017).
[30] B. P. Abbott et. al, Observation of gravitational waves from a binary black hole merger, Phys. Rev. Lett. **116**, 061102 (2016).
[31] T. P. Purdy, R. W. Peterson, and C. A. Regal, Observation of radiation pressure shot noise on a macroscopic object, Science **339**, 801 (2013).
[32] I. Lesanovsky, and W. von Klitzing, Time-averaged adiabatic potentials: versatile matter-wave guides and atom traps, Phys. Rev. Lett. **99**, 083001 (2007).
[33] B. E. Sherlock, M. Gildemeister, E. Owen, E. Nugent, and C. J. Foot, Time-averaged adiabatic ring potential for ultracold atoms, Phys. Rev. A **83**, 043408 (2011).
[34] Y. Guo, R. Dubessy, M. G. de Herve, A. Kumar, T. Badr, A. Perrin, L. Longchambon, and H. Perrin, Supersonic rotation of a superfluid: a long-lived dynamical ring, Phys. Rev. Lett. **124**, 025301 (2020).
[35] O. Morizot, Y. Colombe, V. Lorent and H. Perrin, Ring trap for ultracold atoms, Phys. Rev. A **74**, 023617 (2006).
[36] M. de G. de Herve, Y.Guo, C. De Rossi, A. Kumar, T. Badr, R. Dubessy, L. Longchambon, and H. Perrin, A versatile ring trap for quantum gases, J. Phys. B: At. Mol. Opt. Phys. **54**, 125302 (2021).
[37] K. C. Wright, R. B. Blakestad, C. J Lobb, W. D. Phillips and G. K. Campbell, Threshold for creating excitations in a stirred superfluid ring, Phys. Rev. A **88**, 063633 (2013).
[38] D. Naidoo, K. Aĭt-Ameur, M. Brunel, and A. Forbes, Intra-cavity generation of superpositions of Laguerre-Gaussian beams, Appl. Phys. B **106**, 683 (2012).
[39] See the Supplementary Material for the derivation of the Hamiltonian and the effect of atomic interactions, which includes Refs. [40–47].
[40] D. L. Andrews, *Structured Light and Its Applications: An Introduction to Phase-Structured Beams and Nanoscale Optical Forces*, New York: Academic, 2012.
[41] E. M. Wright, J. Arlt, and K. Dholakia, Toroidal optical dipole traps for atomic Bose-Einstein condensates using Laguerre-Gaussian beams, Phys. Rev. A **63**, 013608 (2000).
[42] C. J. Pethick and H. Smith, *Bose-Einstein Condensation in Dilute Gases*, Cambridge University Press, 2008.
[43] C. C. Gerry and P. L. Knight, *Introductory Quantum Optics*, Cambridge University Press, 2005.
[44] H. J. Metcalf and P. van der Straten, *Laser Cooling and Trapping*, Berlin: Springer, 1999.
[45] E. Tiesinga, C. J. Williams, P. S. Julienne, K. M. Jones, P. D. Lett, and W. D. Phillips, A spectroscopic determination of scattering lengths for sodium atomic collisions, J. Res. Natl. Inst. Stand. Technol. **101**, 505 (1996).
[46] E. X. DeJesus, and C. Kaufman, Routh-Hurwitz criterion in the examination of eigenvalues of a system of nonlinear ordinary differential equations, Phys. Rev. A **35**, 5288 (1987).
[47] Y. D. Wang, S. Chesi, and A. A. Clerk, Bipartite and tripartite output entanglement in three-mode optomechanical systems, Phys. Rev. A **91**, 013807 (2015).
[48] F. Brennecke, S. Ritter, T. Donner, and T. Esslinger, Cavity optomechanics with a Bose-Einstein condensate, Science **322**, 235 (2008).
[49] B. Padhi, and S. Ghosh, Cavity Optomechanics with Synthetic Landau Levels of Ultracold Fermi Gas, Phys. Rev. Lett. **111**, 043603 (2013).
[50] J. Polo, R. Dubessy, P. Pedri, H. Perrin, and A. Minguzzi, Oscillations and decay of superfluid currents in a one-dimensional Bose gas on a ring, Phys. Rev. Lett. **123**, 195301 (2019).
[51] R. Kanamoto, H. Saito, and M. Ueda, Quantum phase transition in one-dimensional Bose-Einstein condensates with attractive interactions, Phys. Rev. A **67**, 013608 (2003).
[52] K. Zhang, W. Chen, M. Bhattacharya, and P. Meystre, Hamiltonian chaos in a coupled BECoptomechanical-cavity system, Phys. Rev. A **81**, 013802 (2010).
[53] M. P. J. Lavery, F. C. Speirits, S. M. Barnett, and M. J. Padgett, Detection of a spinning object using light's orbital angular momentum, Science **341**, 537 (2013).
[54] S. Rotter, F. Brennecke, K. Baumann, T. Donner, C. Guerlin, and T.Esslinger, Dynamical coupling between a Bose-Einstein condensate and a cavity optical lattice, Appl. Phys. B **95**, 213 (2009).
[55] R. S. Schoenfeld, and W. Harneit, Real time magnetic field sensing and imaging using a single spin in diamond,

Phys. Rev. Lett. **106**, 030802 (2011).
[56] M. Lassen, G. Leuchs, and U. L. Andersen, Continuous variable entanglement and squeezing of orbital angular momentum states, Phys. Rev. Lett. **102**, 163602 (2009).
[57] R. Ghobadi, A. R. Bahrampour, and C. Simon, Quantum optomechanics in the bistable regime, Phys. Rev. A **84**, 033846 (2011).